Research Article

URF PUBLISHERS
connect with research world

Journal of Petroleum & Chemical Engineering

https://urfpublishers.com/journal/petrochemical-engineering

Vol: 3 & Iss: 2

Dynamics of Chemoimmunotherapy Models

Lakshmi N Sridhar*

Chemical Engineering Department, University of Puerto Rico, Mayaguez, PR 00681-9046, USA

Citation: Sridhar LN. Dynamics of Chemoimmunotherapy Models. *J Petro Chem Eng* 2025;3(2):85-91.

Received: 19 April, 2025; **Accepted:** 23 May, 2025; **Published:** 26 May, 2025

***Corresponding author:** Lakshmi N Sridhar, Chemical Engineering Department, University of Puerto Rico, Mayaguez, PR 00681-9046, USA

ABSTRACT

Chemoimmunotherapy is chemotherapy combined with immunotherapy. Chemotherapy uses different drugs to kill or slow the growth of cancer cells; immunotherapy uses treatments to stimulate or restore the ability of the immune system to fight cancer. Both chemotherapy and immunotherapy are highly nonlinear processes that several factors affect. The two treatments together would be very highly nonlinear. It is necessary to understand and control this combined treatment. Bifurcation analysis is a powerful mathematical tool used to deal with the nonlinear dynamics of any process. Several factors must be considered and multiple objectives must be met simultaneously. Bifurcation analysis and Mult objective nonlinear model predictive control (MNLMPC) calculations are performed on two chemoimmunotherapy models. The MATLAB program MATCONT was used to perform the bifurcation analysis. The MNLMPC calculations were performed using the optimization language PYOMO in conjunction with the state-of-the-art global optimization solvers IPOPT and BARON. The bifurcation analysis revealed branch and limit points in the two models. The branch and limit points were beneficial because they enabled the Mult objective nonlinear model predictive control calculations to converge to the Utopia point in both the problems, which is the best solution.

Keywords: Bifurcation Optimization; Control; Cancer tumor; Chemotherapy

Background

Buzaid[1], developed strategies for combining chemotherapy and biotherapy in melanoma. De Pillis and Radunskaya[2], developed a mathematical tumor model with immune resistance and drug therapy. Jackson[3], discussed vascular tumor growth and treatment and the consequences of polyclonality, competition and dynamic vascular support. Liu et al[4], investigated cell-mediated immunotherapy which is a new approach to the treatment of malignant glioma. Chaplain[5], discussed several mathematical models in cancer research.

De Pillis and Radunskaya[6], investigated the Immune response to tumor invasion. Schirrmacher, et al[7], discussed several models for immunotherapy and Cancer Vaccines. Arciero, et al[8], developed a mathematical model of tumor-immune evasion and siRNA treatment. Burden, et al[9], applied optimal control techniques to immunotherapy, Chao, et al[10], developed a stochastic model of cytotoxic T cell responses. Matzavinos, Chaplain[11], performed a travelling-wave analysis of a model of the immune response to cancer.

Matzavinos, et al[12], developed mathematical models of the spatiotemporal response of cytotoxic T-lymphocytes to a solid tumor. Garbelli, et al[13], discussed the Melanocyte-specific, cytotoxic T cell responses in vitiligo studying the effective variant of melanoma immunity. Wheeler, et al[14], investigated the Clinical responsiveness of glioblastoma multiforme to chemotherapy after vaccination. Li, et al[15], researched the generation of PRL-3- and PRL-1-specific monoclonal antibodies as potential diagnostic markers for cancer metastases.

Qu, et al[16], investigated the Development of humanized antibodies as cancer therapeutics. De Pillis, et al[17], theoretically

investigated the mixed immunotherapy and chemotherapy of tumors. Malleta and De Pillis[18], developed a cellular automata model of tumor–immune system interactions. De Pillis, et al[19], performed a theoretical investigation of chemotherapy for tumors and Isaeva, et al[20], discussed the different strategies for cancer treatment. Ledzewicz, et al[21], developed optimal controls for a mathematical model of tumor-immune interactions under targeted chemotherapy with immune boost.

Eladdadi, et al[22], developed mathematical models of tumor-immune system dynamics. Wang, et al[23], performed optimal control for a mathematical model for cancer chemotherapy under tumor heterogeneity. Abdel-Wahab, et al[24], discussed the adverse events in cancer immunotherapy. Lai and Friedman[25], discussed the combination therapy of cancer with cancer vaccine and immune checkpoint inhibitors. Ratajczyk, et al[26], performed optimal control for a mathematical model of glioma treatment with oncolytic therapy and TNF-α inhibitors. Guti´errez-Diez and Russo[27], disussed the design of personalized cancer treatments by use of optimal control for the case of chronic myeloid leukemia. Khajanchi[28], investigated the impact of immunotherapy on a glioma immune interaction model. Takacs, et al[29], demonstrated that the modulation of the chemokine/chemokine receptor axis was a novel approach for glioma therapy.

Liu, et al[30], performed a dynamics analysis of a tumor-immune system with chemotherapy. Anderson, et al[31], showed that global stability and parameter analysis reinforce therapeutic targets of PD-L1-PD-1 and MDSCs for glioblastoma. Cherraf, et al[32]. mathematically modelled the tumor–immune system with time delay and diffusion. Luo, et al[33], discussed the optimal treatment strategy for cancer based on mathematical modeling and impulse control theory. Anderson, et al[34], performed optimal control of combination immunotherapy for a virtual murine cohort in a glioblastoma-immune dynamics model.

All optimal control work involving chemoimmunotherapy models involve single-objective optimal control. The main objective of this paper is to perform Mult objective nonlinear model predictive control (MNLMPC) in conjunction with bifurcation analysis for two chemoimmunotherapy models. The two models that will be used are those described in Anderson, et al[34] and the scaled model in Isaeva, et al[20]. This paper is organized as follows. First the model equations are presented. The numerical procedures (bifurcation analysis and Mult objective nonlinear model predictive control (MNLMPC) are then described. This is followed by the results and discussion and conclusions.

Chemoimmunotherapy Models

The two models that are presented in Anderson, et al[34] and the scaled model in Isaeva, et al[20], will be used for the calculations. These models will be briefly described in this section.

Model 1[34]

The model equations are

$$\frac{dc_{val}}{dt} = \lambda_C c_{val}(1-\frac{c_{val}}{c_{\max}}) - \eta t_{val} c_{val}$$

$$\frac{dt_{val}}{dt} = -rt_{val}m_{val} - d_t t_{val} + \frac{(\alpha_T + s_T t_{val} c_{val})}{1+\rho(t_{val}+\varepsilon_C c_{val})(1-u_1(t)t_{val})}$$

$$\frac{dm_{val}}{dt} = s_m c_{val}(1-u_2(t)t_{val}) - d_m m_{val}$$

$c_{val}, t_{val}, m_{val}$ represent the tumor cells, activated T cells and myeloid-derived suppressor cells (MDSCs).

The base parameters are

$$\lambda_c = 0.25;\ c_{max} = 1.45e+07; \eta = 1.27e-07; \alpha_t = 2.45e+06;$$
$$s_t = 5.91e+06; \rho = 0.207; \varepsilon_c = 31.1; r = 1.83e-05; d_t = 0.415;$$
$$s_m = 0.0476; d_m = 0.263;\ u_1 = 0; u_2 = 0;$$

For the bifurcation calculations λ_C was the bifurcation parameter while $u_1 = 0; u_2 = 0$. For the MNLMPC calculations, $\lambda_c = 0.25$ while $u_1; u_2$ are the control variables.

Model 2[20]

The model equations are

$$\frac{dt_{val}}{dt} = -h_1 t_{val} \ln\left(\frac{h_2 t_{val}}{h_1}\right) - h_3 t_{val} l_{val}(2-e^{-i_{val}}) - m_1 t_{val}(2-e^{-i2_{val}})(1-e^{-c_{val}})$$

$$\frac{dl_{val}}{dt} = h_4 + h_5 l_{val} I2_{val} - l_{val} - m_2 l_{val}(2-e^{-i2_{val}})(1-e^{-c_{val}})$$

$$\frac{dI2_{val}}{dt} = m_3(t) + \left(\frac{h_6 t_{val}}{t_{val}+h_9}\right) - h_7 l_{val} I2_{val} - h_8 t_{val} I2_{val}$$

$$\frac{dC_{val}}{dt} = m_4(t) - m_5 c_{val}$$

$$\frac{dI_{val}}{dt} = m_6(t) - m_7 I_{val}$$

$t_{val}, l_{val}, I2_{val}, c_{val}, I_{val}$ represent the dimensionless tumor cells, Cytotoxic T Lymphocytes, Interleukin-2, chemotherapeutic drug (C) and Interferon-alpha.

The scaled model parameters are

$h_1 = 0.3939, h_2 = 0.0909, h_3 = 1.5000, h_4 = 0.2458, h_5 = 0.6061, h_6 = 3.6364, h_7 = 1.0091,$
$h_8 = 6.3636, h_9 = 0.0300, m_1 = 2.7273, m_2 = 1.8182, m_5 = 19.3939, m_7 = 5.1515.$

m_3, m_4, m_6 were taken as individual bifurcation parameters (one at a time, with the other two being 0) and collectively as control parameters for the MNLMPC calculations.

Numerical Procedures

Bifurcation analysis

The MATLAB software MATCONT is used to perform the bifurcation calculations. Bifurcation analysis deals with multiple steady-states and limit cycles. Multiple steady states occur because of the existence of branch and limit points. Hopf bifurcation points cause limit cycles. A commonly used MATLAB program that locates limit points, branch points and Hopf bifurcation points is MATCONT[35,36]. This program detects Limit points (LP), branch points (BP) and Hopf bifurcation points(H) for an ODE system.

$$\frac{dx}{dt} = f(x,\alpha)$$

$x \in R^n$ Let the bifurcation parameter be α Since the gradient is orthogonal to the tangent vector,

The tangent plane at any point $W = [w_1, w_2, w_3, w_4, ...w_{n+1}]$ must satisfy

$$Aw = 0$$

Where A is

$$A = [\partial f / \partial x \quad | \partial f / \partial \alpha]$$

where $\partial f / \partial x$ is the Jacobian matrix. For both limit and branch points, the matrix $[\partial f / \partial x]$ must be singular. The n+1 th component of the tangent vector $w_{n+1} = 0$ for a limit point (LP)and for a branch point (BP) the matrix $\begin{bmatrix} A \\ w^T \end{bmatrix}$ must be singular. At a Hopf bifurcation point,

$$\det(2 f_x(x,\alpha) @ I_n) = 0$$

@ indicates the bialternate product while I_n is the n-square identity matrix. Hopf bifurcations cause limit cycles and should be eliminated because limit cycles make optimization and control tasks very difficult. More details can be found in Kuznetsov[37,38] and Govaerts[39].

Mult objective nonlinear model predictive control (MNLMPC)

Flores Tlacuahuaz, et al[40], developed a Mult objective nonlinear model predictive control (MNLMPC) method that is rigorous and does not involve weighting functions or additional constraints. This procedure is used for performing the MNLMPC calculations Here $\sum_{t_{i=0}}^{t_i=t_f} q_j(t_i)$ (j=12.n) represents the variables that need to be minimized/maximized simultaneously for a problem involving a set of ODE

$$\frac{dx}{dt} = F(x,u)$$

t_f being the final time value and n the total number of objective variables and u the control parameter. This MNLMPC procedure first solves the single objective optimal control problem independently optimizing each of the variables $\sum_{t_{i=0}}^{t_i=t_f} q_j(t_i)$ individually. The minimization/maximization of $\sum_{t_{i=0}}^{t_i=t_f} q_j(t_i)$ will lead to the values q_j^* . Then the optimization problem that will be solved is

$$\min (\sum_{j=1}^{n} (\sum_{t_{i=0}}^{t_i=t_f} q_j(t_i) - q_j^*))^2$$

$$subject\ to\ \frac{dx}{dt} = F(x,u);$$

This will provide the values of u at various times. The first obtained control value of u is implemented and the rest are discarded. This procedure is repeated until the implemented and the first obtained control values are the same or if the Utopia point where ($\sum_{t_{i=0}}^{t_i=t_f} q_j(t_i) = q_j^*$ for all j) is obtained.

Pyomo[41], is used for these calculations. Here, the differential equations are converted to a Nonlinear Program (NLP) using the orthogonal collocation method The NLP is solved using IPOPT[42] and confirmed as a global solution with BARON[43].

The steps of the algorithm are as follows

- Optimize $\sum_{t_{i=0}}^{t_i=t_f} q_j(t_i)$ and obtain q_j^* at various time intervals t_i. The subscript *i* is the index for each time step.
- Minimize $(\sum_{j=1}^{n} (\sum_{t_{i=0}}^{t_i=t_f} q_j(t_i) - q_j^*))^2$ and get the control values for various times.
- Implement the first obtained control values
- Repeat steps 1 to 3 until there is an insignificant difference between the implemented and the first obtained value of the control variables or if the Utopia point is achieved. The Utopia point is when $\sum_{t_{i=0}}^{t_i=t_f} q_j(t_i) = q_j^*$ for all j.

Sridhar[44], proved that the MNLMPC calculations to converge to the Utopia solution when the bifurcation analysis revealed the presence of limit and branch points. This was done by imposing the singularity condition on the co-state equation[45]. If the minimization of q_1 lead to the value q_1^* and the minimization of q_2 lead to the value q_2^* The MNLPMC calculations will minimize the function $(q_1 - q_1^*)^2 + (q_2 - q_2^*)^2$. The Mult objective optimal control problem is

$$\min \quad (q_1 - q_1^*)^2 + (q_2 - q_2^*)^2 \quad subject\ to\ \frac{dx}{dt} = F(x,u)$$

Differentiating the objective function results in

$$\frac{d}{dx_i}((q_1 - q_1^*)^2 + (q_2 - q_2^*)^2) = 2(q_1 - q_1^*)\frac{d}{dx_i}(q_1 - q_1^*) + 2(q_2 - q_2^*)\frac{d}{dx_i}(q_2 - q_2^*)$$

The Utopia point requires that both $(q_1 - q_1^*)$ and $(q_2 - q_2^*)$ are zero. Hence

$$\frac{d}{dx_i}((q_1 - q_1^*)^2 + (q_2 - q_2^*)^2) = 0$$

the optimal control co-state equation (Upreti; 2013) is

$$\frac{d}{dt}(\lambda_i) = -\frac{d}{dx_i}((q_1 - q_1^*)^2 + (q_2 - q_2^*)^2) - f_x \lambda_i; \quad \lambda_i(t_f) = 0$$

λ_i is the Lagrangian multiplier. t_f is the final time. The first term in this equation is 0 and hence

$$\frac{d}{dt}(\lambda_i) = -f_x \lambda_i; \lambda_i(t_f) = 0$$

At a limit or a branch point, for the set of ODE $\frac{dx}{dt} = f(x,u)$ f_x is singular. Hence there are two different vectors-values for $[\lambda_i]$ where $\frac{d}{dt}(\lambda_i) > 0$ and $\frac{d}{dt}(\lambda_i) < 0$. In between there is a vector $[\lambda_i]$ where $\frac{d}{dt}(\lambda_i) = 0$. This coupled with the boundary condition $\lambda_i(t_f) = 0$ will lead to $[\lambda_i] = 0$ This makes the problem

an unconstrained optimization problem and the only solution is the Utopia solution.

Hopf bifurcations cause unwanted oscillatory behavior and limit cycles. The tanh activation function (where a control value u is replaced by) $(u \tanh u/\varepsilon)$ is commonly used in neural nets[46-48] and optimal control problems[49], to eliminate spikes in the optimal control profile. Hopf bifurcation points cause oscillatory behavior. Oscillations are similar to spikes and the results in Sridhar demonstrate that the tanh factor also eliminates the Hopf bifurcation by preventing the occurrence of oscillations. Sridhar[50], explained with several examples how the activation factor involving the tanh function successfully eliminates the limit cycle causing Hopf bifurcation points. This was because the tanh function increases the time period of the oscillatory behavior, which occurs in the form of a limit cycle caused by Hopf bifurcations.

Results and Discussion

In model 1, for the bifurcation calculations λ_C was the bifurcation parameter and a branch point BP was found at $[c_{val}, t_{val}, m_{val}, \lambda_c]$ == (14500000, 0, 2624334.6, 0). Figure 1a shows the bifurcation diagram with this branch point. For the MNLMPC calculation, with u1 and u2 as the control variables. $\sum_{t_i=0}^{t_i=t_f} mval_j(t_i)$ was minimized, leading to a value of 0 and $\sum_{t_i=0}^{t_i=t_f} cval_j(t_i)$ was minimized also resulting in a value of 0. The overall optimal control problem will involve the minimization of $(\sum_{t_i=0}^{t_i=t_f} mval_j(t_i)-0)^2+(\sum_{t_i=0}^{t_i=t_f} cval_j(t_i)-0)^2$ subject to the ODE describing Model 1. This minimization resulted in the Utopia point (0) confirming the analysis of Sridhar[34], which showed that the presence of a branch point enables the MNLMPC calculations to reach the best possible (Utopia) solution. The first of the control variables is implemented and the rest are discarded. The process is repeated until the difference between the first and second values of the control variables are the same. This MNLMPC control values of u1 and u2 were 4.824e-07 and 0.4878. The various MNLMPC profiles are shown in **(Figure 1a and 1c)**. The obtained control profile of s exhibited noise **(Figure 1d)**. This was remedied using the Savitzky-Golay Filter. The smoothed-out version of this profile is shown in **(Figure 1e)**.

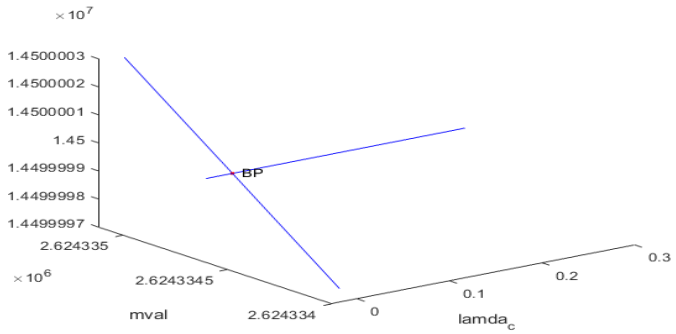

Figure 1a: Bifurcation Diagram for model 1.

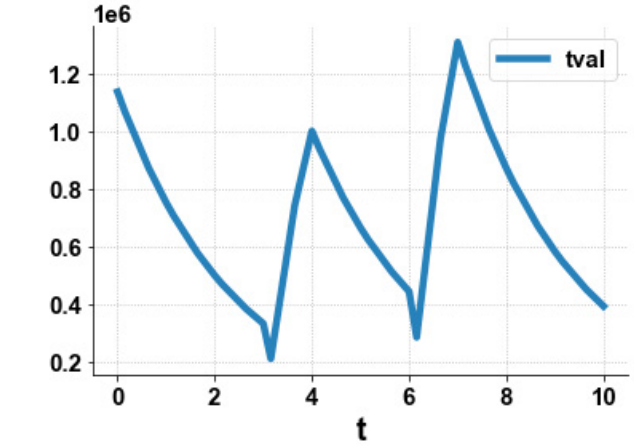

Figure 1b: tval vs t (MNLMPC model 1).

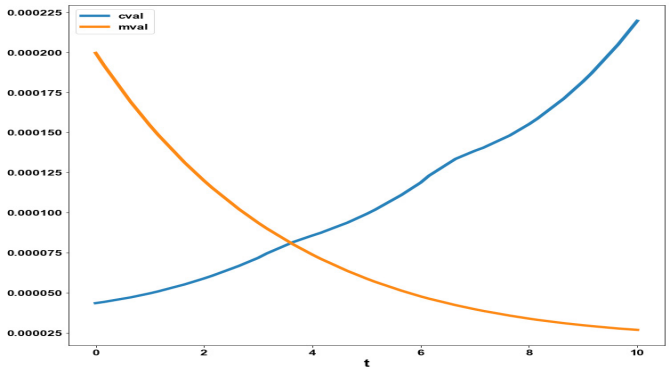

Figure 1c: cval, mval vs t (MNLMPC model 1).

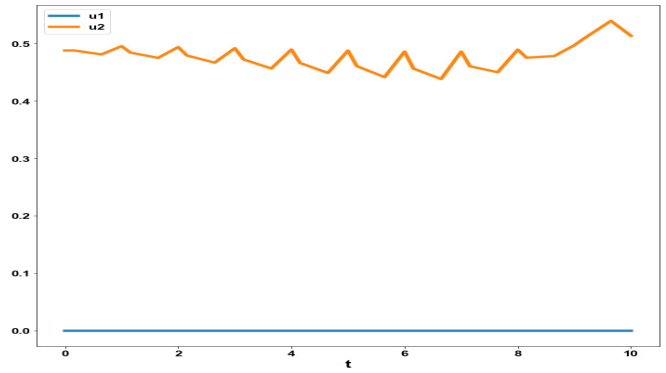

Figure 1d: u1, u2 vs t (MNLMPC model 1) some noise is observed.

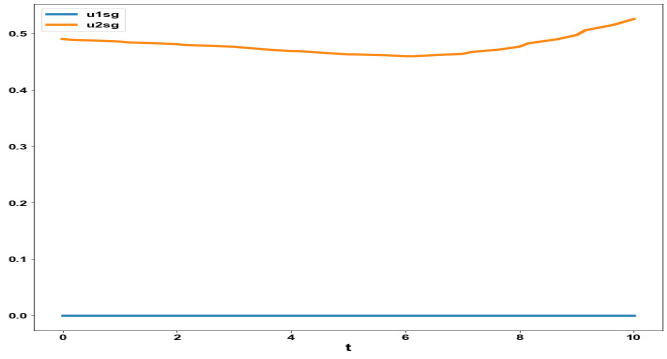

Figure 1e: u1, u2 vs t (MNLMPC model 1) with Savitsky Golay filter

In model 2, m_3, m_4, m_6 each, when used as a bifurcation parameter, revealed the existence of a limit point. The coordinates for these $(t_{val}, l_{val}, I2_{val}, c_{val}, I_{val}, m_j)$ limit points j = 3,4,6 is (0.8622, 0.4240, 0.6935, 0.0, 0.0, 0.588); (0.5895, 0.3931,

0.8341, 0.047, 0.0, 0.9116) and (0.7542, 0.4139, 0.6703, 0.0, 0.1156, 0.5957). **(Figure 2a, 2b and 2c)** show the bifurcation diagrams for model 2.

For the MNLMPC calculation, with m3 m4 and m6 s the control variables $\sum_{t_i=0}^{t_i=t_f} tval_j(t_i)$ was minimized, leading to a value of 3.45e-05 and $\sum_{t_i=0}^{t_i=t_f} lval_j(t_i)$ was maximized resulting in a value of 10.951. The overall optimal control problem will involve the minimization of $(\sum_{t_i=0}^{t_i=t_f} tval_j(t_i) - 3.45e-05)^2 + (\sum_{t_i=0}^{t_i=t_f} lval_j(t_i) - 10.951)^2$ subject to the ODE describing Model 2. This minimization resulted in the Utopia point (0), confirming the analysis of Sridhar[34], which showed that the presence of a branch point enables the MNLMPC calculations to reach the best possible (Utopia) solution. The first of the control variables is implemented and the rest are discarded. The process is repeated until the difference between the first and second values of the control variables are the same. This MNLMPC control values of m3 m4 and m6 were 0.3491, 2.99977, 7.27841e-06. The various MNLMPC profiles are shown in **(Figure 2d and 2e).** The obtained control profile of s exhibited noise **(Figure 2f)**. This was remedied using the Savitzky-Golay Filter. The smoothed-out version of this profile is shown in **(Figure 2g)**.

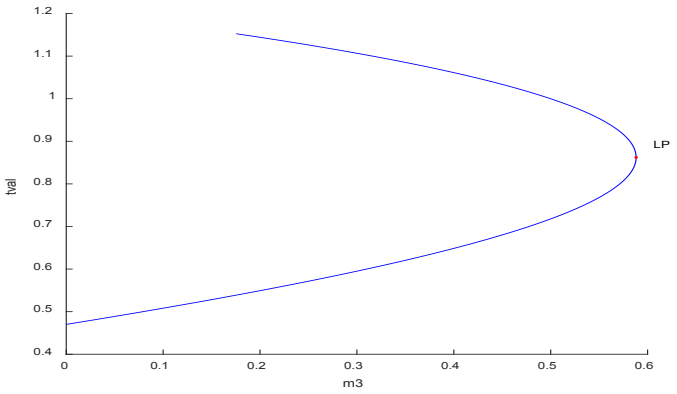

Figure 2a: Bifurcation Diagram for model 2 (m3 as bifurcation parameter).

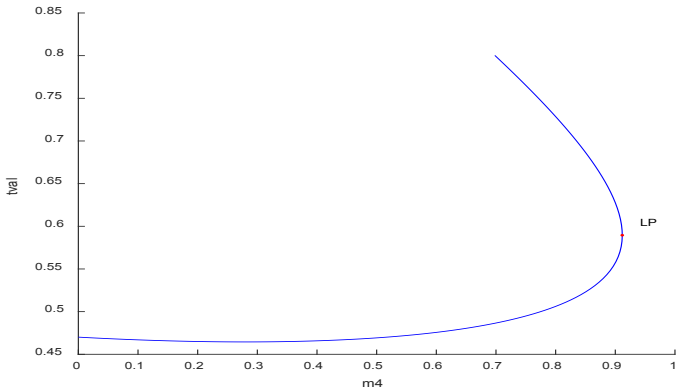

Figure 2b: Bifurcation Diagram for model 2 (m4 as bifurcation parameter)

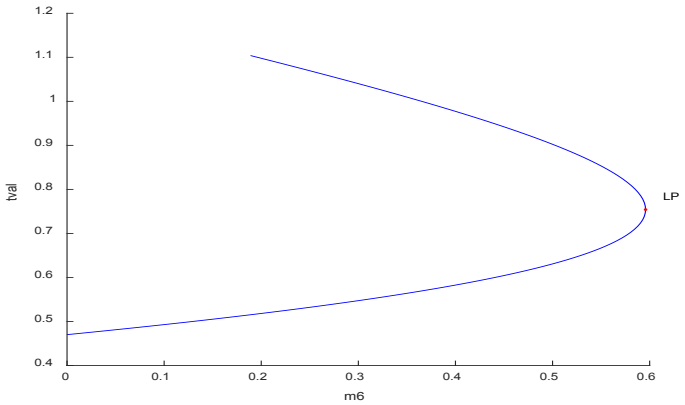

Figure 2c: Bifurcation Diagram for model 2 (m6 as bifurcation parameter).

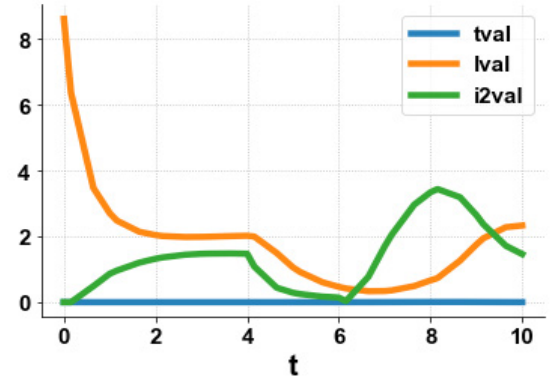

Figure 2d: tval, lval, i2val vs t (MNLMPC model 2).

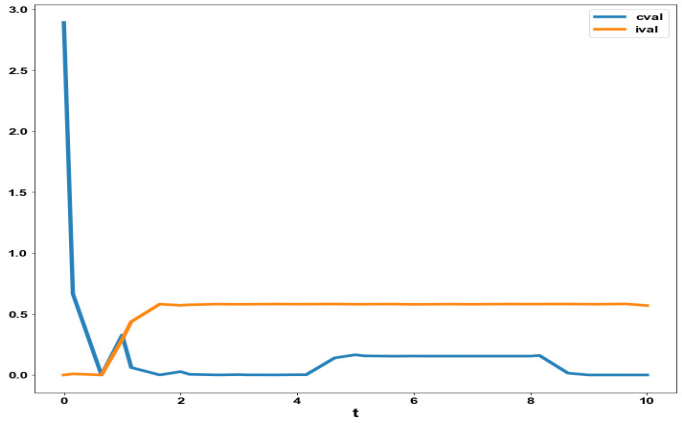

Figure 2e: cval, ival vs t (MNLMPC model 2).

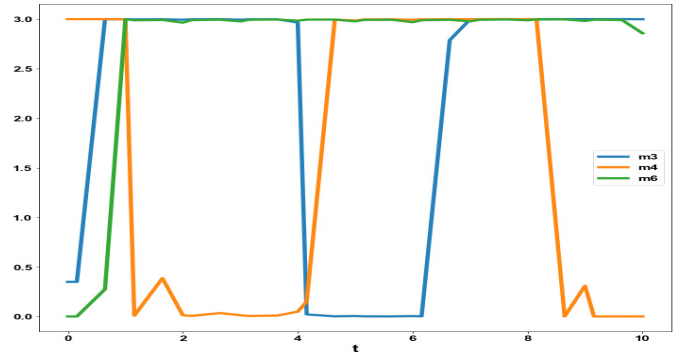

Figure 2f: m3 m4 m6 vs t (MNLMPC model 1) some noise is observed.

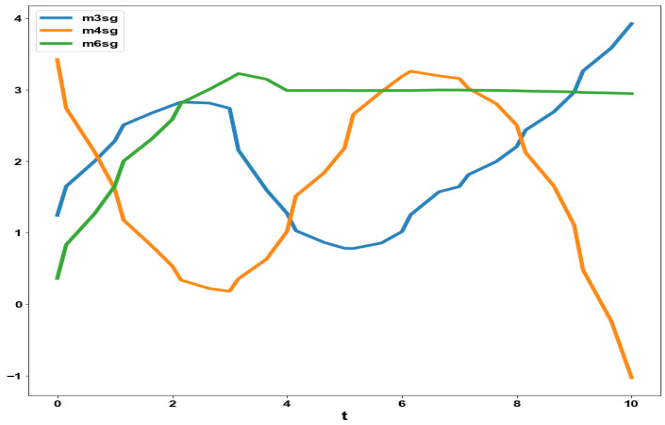

Figure 2g: m3, m4, m6 vs t (MNLMPC model 2) with Savitsky-Golay filter.

Conclusion

Multiobjective nonlinear model predictive control calculations were performed along with bifurcation analysis on two chemoimmunotherapy models. The bifurcation analysis revealed the existence of limit and branch points that produced multiple steady-state solutions originating from a singular point. The limit and branch points are very beneficial as they caused the multiojective nonlinear model predictive calculations to converge to the Utopia point (the best possible solution) in both models.

Data Availability Statement

All data used is presented in the paper.

Conflict of Interest

The author, Dr. Lakshmi N Sridhar has no conflict of interest.

Acknowledgement

Dr. Sridhar thanks Dr. Carlos Ramirez and Dr. Suleiman for encouraging him to write single-author papers.

References

1. Buzaid AC. Strategies for combining chemotherapy and biotherapy in melanoma, Cancer Control 2000;7(2):185-197.
2. De Pillis LG, Radunskaya A. A mathematical tumor model with immune resistance and drug therapy: an optimal control approach. J Theoretical Med 2001;3:79-100.
3. Jackson TL. Vascular tumor growth and treatment: consequences of polyclonality, competition and dynamic vascular support. J Math Biol 2002;44:201-226.
4. Liu Y, Ng Y, Lillehei KO. Cell mediated immunotherapy: a new approach to the treatment of malignant glioma, Cancer Control 2003;10:138-147.
5. Chaplain MAJ. Mathematical models in cancer research, in: The Cancer Handbook, Nature publishing group, Chapter 60 2003;60:937-951.
6. De Pillis LG, Radunskaya AE. Immune response to tumor invasion, in: Computational Fluid and Solid Mechanics, K. Bathe, eds. Cambridge: MIT Press, MA 2003:1661-1668.
7. Schirrmacher V, Umansky V, Linder M, Müerköster S, Rocha M. Models for immunotherapy and Cancer Vaccines, in: The Cancer Handbook, Chapter 68 Nature publishing group 2003:1055-1068.
8. Arciero JC, Kirschner DE, Jackson TL. A mathematical model of tumor-immune evasion and siRNA treatment. Disc Cont Dyn Syst-B 2004;4:39-58.
9. Burden T, Ernstberger J, Renee Fister K. Optimal control applied to immunotherapy, Discrete and Continuous dynamical systems-series B 2004;4:135-146.
10. Chao DL, Davenport MP, Forrest S, Perelson AS. A stochastic model of cytotoxic T cell responses. J Theoretical Bio 2004;228:227-240.
11. Matzavinos A, Chaplain MAJ. Travelling-wave analysis of a model of the immune response to cancer. C R Biol 2004;327(11):995-1008.
12. Matzavinos A, Chaplain MAJ, Kuznetsov VA. Mathematical modelling of the spatiotemporal response of cytotoxic T-lymphocytes to a solid tumour. Mathematical Med Bio 2004;2:1-34.
13. Garbelli S, Mantovani S, Palermo B, Giachino C. Melanocyte-specific, cytotoxic T cell responses in vitiligo: the effective variant of melanoma immunity. Pigment Cell Res 2005;18:234-242.
14. Wheeler CJ, Asha D, Genatao L, Yu JS, Black KL. Clinical responsiveness of glioblastoma multiforme to chemotherapy after vaccination. Clin Cancer Res 2005;10:5316-5326.
15. Li J, Guo K, Koh VW, et al. Generation of PRL-3- and PRL-1-specific monoclonal antibodies as potential diagnostic markers for cancer metastases. Clin Cancer Res 2005;11(6):2195-2204.
16. Qu Z, Griffiths GL, Wegener WA. Development of humanized antibodies as cancer therapeutics, Methods 2005;36(1):84-95.
17. De Pillis LG, Gu W, Radunskaya AE. Mixed immunotherapy and chemotherapy of tumors: modeling, applications and biological interpretations. J of Theoretical Bio 2006;238(4):841-862.
18. Malleta DG, de Pillis LG. A cellular automata model of tumor–immune system interactions. J Theor Biol 2006;239:334-350.
19. De Pillis LG, Gu W, Fister KR, et al. Chemotherapy for tumors: an analysis of the dynamics and a study of quadratic and linear optimal controls, Mathematical Biosciences 2007;209:292-315.
20. Isaeva OG, Osipov VA. Different Strategies for Cancer Treatment: Mathematical Modelling. Computational Mathematical Methods in Med 2009;10(4):253-272.
21. Ledzewicz U, Mosalman MSF, Sch¨attler H. Optimal controls for a mathematical model of tumor-immune interactions under targeted chemotherapy with immune boost. Discrete Cont Dyn B 2013;18;1031-1051.
22. Eladdadi A, Kim P, Mallet D, et al. Mathematical models of tumor-immune system dynamics. Springer, New York, NY, 2014;107.
23. Wang S, Sch¨attler H. Optimal control of a mathematical model for cancer chemotherapy under tumor heterogeneity. Math. Biosci Eng 2016;13:1223-1240.
24. Abdel-Wahab N, Alshawa A, Suarez-Almazor ME. Adverse events in cancer immunotherapy. Adv Exp Med Biol 2017:155-174.
25. Lai X, Friedman A. Combination therapy of cancer with cancer vaccine and immune checkpoint inhibitors: A mathematical model. PLoS One 2017;12:e0178479.
26. Ratajczyk E, Ledzewicz U, Sch¨attler H. Optimal control for a mathematical model of glioma treatment with oncolytic therapy and TNF-α inhibitors. J Optim Theory Appl 2018;176:456-477.
27. Guti´errez-Diez PJ, Russo J. Design of personalized cancer treatments by use of optimal control problems: The case of chronic myeloid leukemia. Math Biosci Eng 2020;17:4773-4800.
28. Khajanchi S. The impact of immunotherapy on a glioma immune interaction model. Chaos Soliton Fract 2021;152:111346.

29. Takacs GP, Flores-Toro JA, Harrison JK. Modulation of the chemokine/chemokine receptor axis as a novel approach for glioma therapy. Pharmacol Ther 2021;222:107790.
30. Liu H, Yang H, Yang L. Dynamics analysis in a tumor-immune system with chemotherapy. Chin Phys B 2021;30:058201.
31. Anderson HG, Takacs GP, Harris DC, et al. Global stability and parameter analysis reinforce therapeutic targets of PD-L1-PD-1 and MDSCs for glioblastoma. J Math Biol 2023;88:10.
32. Cherraf A, Li M, Moulai-Khatir A, Hamidaoui M. Mathematical modeling of the tumor–immune system with time delay and diffusion. Axioms 2023;12:184.
33. Luo W, Tan X, Shen J. Optimal treatment strategy for cancer based on mathematical modeling and impulse control theory. Axioms 2023;12:916.
34. Anderson HG, Takacs GP, Harrison JK, Rong L, Stepien L. Optimal control of combination immunotherapy for a virtual murine cohort in a glioblastoma-immune dynamics model. J Theoretical Bio 2024;595:111951.
35. Dhooge A, Govearts W, Kuznetsov AY. MATCONT: A Matlab package for numerical bifurcation analysis of ODEs. ACM transactions on Mathematical software 2003;29(2):141-164.
36. Dhooge A, Govaerts W, Kuznetsov YA, Mestrom W, Riet AM. CL_MATCONT; A continuation toolbox in Matlab 2004.
37. Kuznetsov YA. Elements of applied bifurcation theory. Springer, NY 1998.
38. KuznetsovYA. Five lectures on numerical bifurcation analysis. Utrecht University, NL 2009.
39. Govaerts WJF. Numerical Methods for Bifurcations of Dynamical Equilibria. SIAM 2000.
40. Flores-Tlacuahuac A, Morales P, Toledo MR. Multiobjective Nonlinear model predictive control of a class of chemical reactors. I & EC research 2012:5891-5899.
41. William EH, Laird CD, Watson JP, et al. Pyomo - Optimization Modeling in Python. Second Edition 67.
42. Wächter A, Biegler L. On the implementation of an interior-point filter line-search algorithm for large-scale nonlinear programming. Math Program 2006;106:25-57.
43. Tawarmalani M, Sahinidis NV. A polyhedral branch-and-cut approach to global optimization. Mathematical Programming 2005;103(2), 225-249,
44. Sridhar LN. Coupling Bifurcation Analysis and Multiobjective Nonlinear Model Predictive Control. Austin Chem Eng 2024;10(3):1107.
45. Ranjan US. Optimal control for chemical engineers. Taylor and Francis 2013.
46. Dubey SR, Singh SK, Chaudhuri BB. Activation functions in deep learning: A comprehensive survey and benchmark. Neurocomputing 2022;503:92-108.
47. Kamalov AF, Safaraliev NM, Cherukuri AK, Zgheib R. Comparative analysis of activation functions in neural networks. 2021 28th IEEE International Conference on Electronics, Circuits and Systems (ICECS), Dubai, United Arab Emirates 2021:1-6.
48. Szandała T. Review and Comparison of Commonly Used Activation Functions for Deep Neural Networks 2020.
49. Sridhar LN. Bifurcation Analysis and Optimal Control of the Tumor Macrophage Interactions. Biomed J Sci Tech Res 2023;53(5).
50. Sridhar LN. Elimination of oscillation causing Hopf bifurcations in engineering problems. J Applied Math 2024;2:1826.